2. Background Theory:

This Chapter presents the Theoretical Background of radiation Therapy physics, which includes the production of clinically useful beams, the biological effect of radiation the Radiotherapy treatment planning system including its Calculation algorithms, general Dosimetry concepts, and other related topics.

2.1 Radiation Therapy:

Cancer is one of the most prominent causes of death worldwide, having accounted for approximately 12.5% of total deaths in 2002 (over 7 million people) (WHO,report4,2004).In 2009 the first National Population based Cancer Registry (NCR) was established in Sudan, from 2010 they found 6771 new cancer cases were registered. 3646 (53.8%) of those cases were women and 3125 (46.2%) were men (Cancer Registry Center, 2014).

The term ‘cancer’ refers to various diseases characterized by two symptoms: the unregulated proliferation of cells and the spread of these cells through the body by invasion and/or metastasis. Cell proliferation typically results in the development of neoplasms (more commonly known as tumors). Without the capability to spread, a tumor might not pose a risk, and is considered benign.

Cancer develops as a result of genetic abnormalities in proto-oncogenes and tumor suppressor genes which translate genetic code into proteins that promote and suppress cell growth respectively. These abnormalities can be the result of mutagen altering genetic information or a spontaneous error in DNA replication. Substances responsible for these mutations are known as carcinogens.

The location and stage of a tumor determines the available treatment options: surgical removal, chemotherapy, hormone therapy, immunotherapy, and radiation therapy. Radiation therapy is the main modalities where cure is the aim.

Treatments may also be delivered as part of palliative care, where the aim is to improve the quality of life of the patient. Radiation therapy is a treatment modality in which a therapeutic dose of ionizing radiation is delivered to a tumor. This radiation disrupts the malignant tissue, with the desired result being cell death or an impairment to cellular division.

The dose or level of radiation is prescribed by an oncologist, and depends on the size, stage and location of the tumor, and the use of any other treatment modalities. The term radiotherapy does not encompass the use of nonionizing radiation to excite radiosensitisers (such as in photodynamic therapy) (C. M. Philipp and H.-P. Berlien, 2006).

Tumors cannot be treated in isolation; inevitably normal tissue will also be damaged. The aim of radiation therapy is to maximize the dose to the tumor, while minimizing the dose to healthy tissue (reducing complication likelihood), that is to find the greatest therapeutic ratio. This chapter will discuss beam delivery, the physics of radiotherapy, radiobiology and the treatment planning process.

2.2 Radiation Delivery:

High energy photons, electrons and protons are all capable of ionizing atoms or molecules and can be used for radiation therapy. Radiation can be delivered via an external beam, an internal sealed source (brachytherapy) or an injected or ingested radioisotope.

Photon based external beam therapy (sometimes called teletherapy or Photon therapy) is the most frequently used clinical treatment modality. Radioactive sources, orthovoltage units or linear accelerators can be used to deliver this beam. Electron based therapy is generally reserved for superficial treatment, due to the short range of electrons. Hadron based therapies are uncommon clinically because, while they offer a highly depth-conformal dose, delivery is more complicated and expensive.

This research is focused on the delivery of photon-based external beam radiotherapy treatments using linear accelerators (linacs), such as the one displayed in *Figure 2.1*, which are used for the production of a high energy electron and photon beams and the adaptation of these beams for treatment use. Generally these devices are able to provide both photon and electron beams of various energies ranging from 4 to 15 MeV. Particle acceleration is required to obtain these energies which exceed those provided by conventional x-ray tubes.

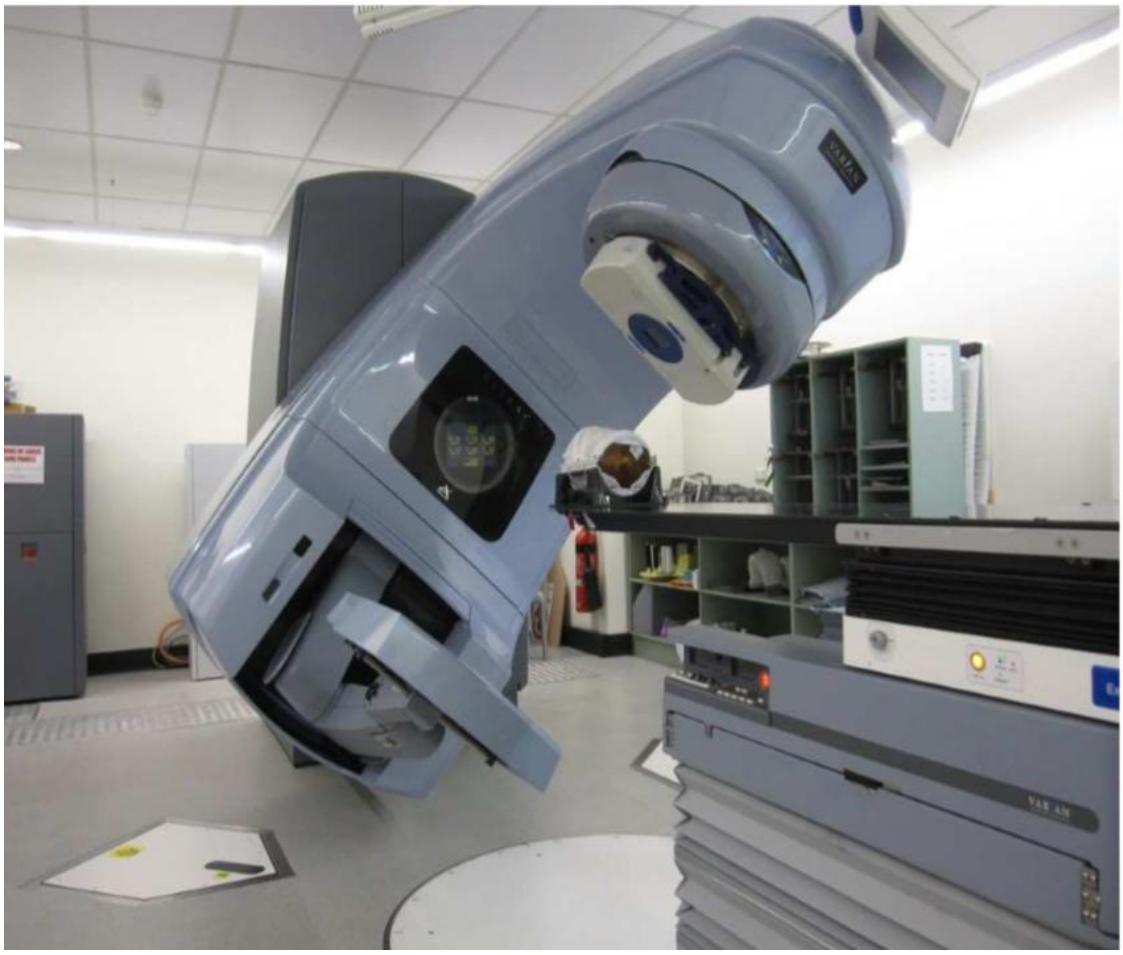

Figure 2.1: Photograph of a Varian MDX Clinac® 2100C linear accelerator, with the gantry currently rotated approximately 60^{o} clockwise. The patient couch can be seen in the foreground in the lower right corner of the image, and the treatment head can be seen above this.

n accelerating waveguide structure is used to accelerate a stream of electrons (supplied by an electron gun, which is a heated cathode) to the specified energy. The acceleration is provided by electric fields, associated with resonating microwaves inside the tuned cavity. Steering and focusing solenoid coils are used to ensure the electrons are retained in focus, direction, and position within the guide (P. Metcalfe, T. Kron, and P. Hoban,2007).

These accelerating waveguide systems are frequently too large to be located on the treatment axis (that is perpendicular to the patient) and so the beam must be bent after acceleration. The bending magnet system responsible for this refocuses the beam, such that the final output is near-monoenergetic (no greater than 5% of nominal peak energy)(P. Metcalfe, T. Kron, and P. Hoban,2007) and near-monodirectional.This electron beam enters the 'treatment head' of the linac, which is responsible for adapting it into a therapeutically useful beam. The production of a clinicalphoton beam involves: a target, a primary (fixed) collimator, a flattening filter, and a monitor ionization chamber and secondary collimators.

Some of these components are contained within a carousel, to be rotated out, for example, when an electron beam is required. The secondary collimators are patient specific; they are adjusted for a particular treatment strategy, while the other components are treatment-independent and fixed for a given mode of operation. *Figure 2.2* illustrates an example treatment head structure, containing the previously mentioned components (and a mirror for reflecting light through the secondary collimators, which can be used for positioning the patient).

The electrons beam which to reiterate is near-monodirectional and it incident on the target. The cross sectional area of incidence is proportional to the focal spot size, the cross sectional area of the volume which produces x-rays. Bremsstrahlung production, where photons are produced when electrons experience deceleration due to charged particle deflection, resulting in a broad photon beam.

To obtain the required fluency (a measure of the number of particles intersecting a unit area), a high-Z target material such as tungsten is frequently used. There is usually a low-Z material below this for electron absorption (resulting in higher x-ray beam energy). The target typically has a thickness of less than 2 cm and depends on the beam energy. The divergence of the resultant beam is restricted by a conical aperture known as the primary collimator, the dimensions of which define an approximately 60 cm diameter circular field at 100 cm from the source (i.e. from the target).

The fluency of the broad bremsstrahlung radiation beam is non-uniformspatiallythe photon beam is forward peaked, and the photon energies are inversely proportional to the angular deviation from the incident electron beam; the net effect is a prevalence of higher energy photons concentrated along the central axis of the beam. To obtain a uniform field which is useful for treatment a 'flattening filter' is used. The filter is thickest along the central axis, so that particles in the center of the field a greater attenuation. This is often made out of tungsten or steel (P. Metcalfe, T. Kron, and P. Hoban,2007).

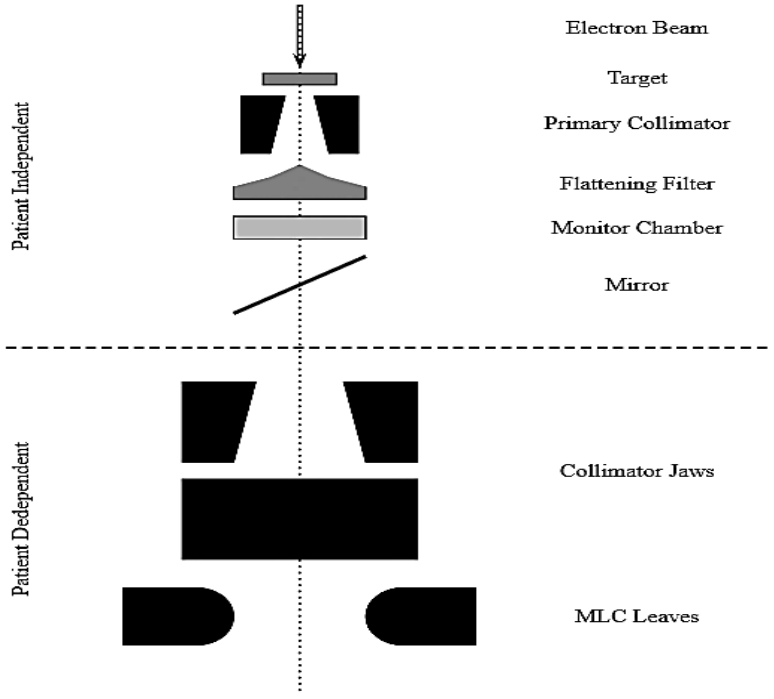

Figure2.2: Treatment head geometry (not to scale)

The next component is the monitor chamber which does not directly affect the beam. It usually consists of two parallel plate ionization chamber; radiation detectors designed to measure the intensity of ionization in the gas medium between the plates.

Ions and dissociated electrons are produced when the high energy photons interact with the gas and attracted towards the polarized plates, resulting in a measurable current. This current indicates the 'output' of the accelerator and providing feedback which can be used to monitor production.

There are two chambers orientated such that one is rotated 90° to the other; this allows a simple monitoring of beam symmetry and provides redundancy in case of error [26]. Unlike the vented chambers commonly used in quality assurance measurements, these chambers are sealed so that the response is not dependent on temperature and pressure.

The broad photon beam is uniform and monitored, suitable for therapeutic use. The secondary collimators, opposing pairs of metal blocks known as jaws, are responsible for restricting the size and shape of the incident radiation field.

The jaws are typically thick enough to limit radiation transmission (for example 8 cm thick for tungsten or lead alloys)(P. Metcalfe, T. Kron, and P. Hoban,2007) and are often designed in such a way that the edge of the jaw matches the angle of beam divergence. The two opposing pairs of jaws can be rotated within the treatment head. The opposing jaws in each pair are independently driven, allowing asymmetric fields.

The field can be further shaped using a multileaf collimator (MLC) system, an array of narrow interleaved collimators that can be driven separately, providing irregular field shapes. This allows what is known as 3D conformal therapy.

2.3 Radiation Physics:

The first step in describing the effect of radiation on a patient is to examine the properties of the linear accelerator output, most importantly the energy distribution. *Figure 2.3* presents the energy fluence below the treatment head of a Linear accelerator operating at 6 MV. This energy describes the nominal acceleration voltage of the electron beam. The upper limit of the photon energy is determined by the electron acceleration (in this case a value near the nominal 6 MeV). Low energy photons are effectively filtered out of the beam by the target and flattening filter. In this example particles with energies between 1 .5 and 2 MeV are the most prevalent.

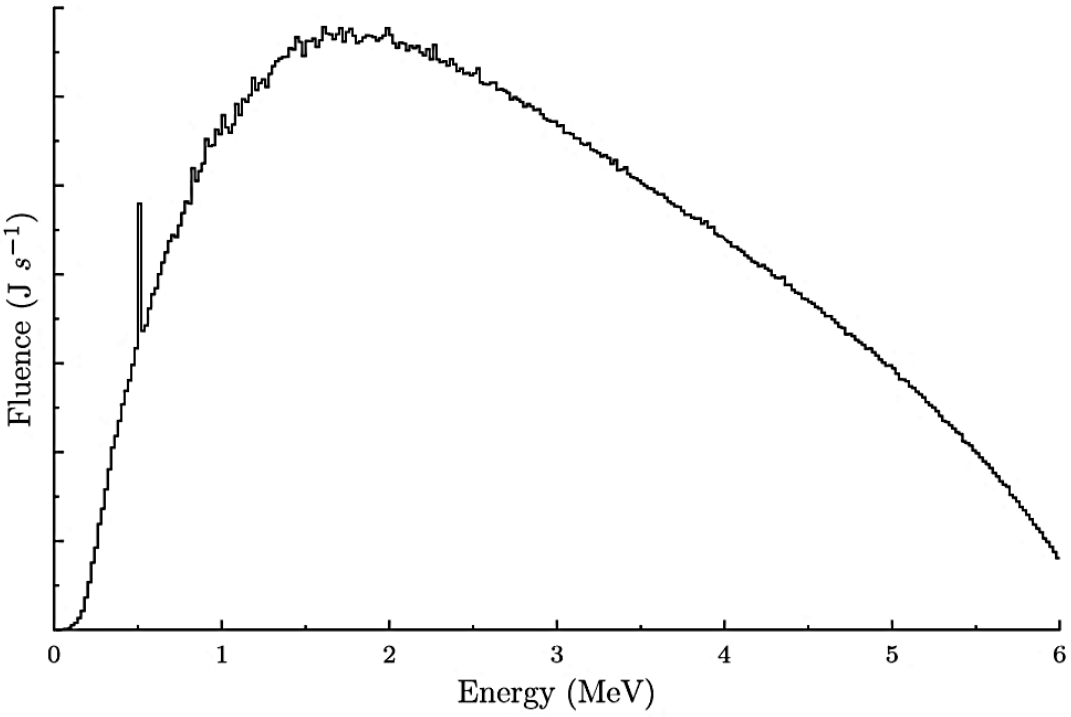

Figure 2.3: Energy fluence beneath treatment head of a 6 MV linear accelerator

These energies determine the type of ionization interactions occurring in the patient. The interactions experienced by these photons can be probabilistically described usingphysical cross sections.Cross sections arc expressed in terms of the effective area occupied by particles (measured in barns, which are equivalent to 10^{-24} cm^2) for a unit solid angle for a given interaction type.

Figure 2.4 presents the photon cross sections in water for energies from 0.01 and 10 MeV for the three most likely ionizing interactions: the photoelectric effect, Compton scattering and pair production.

2.3.1 Photon Interactions:

The photoelectric effect occurs when an electron, known as the 'photoelectron', is emitted by an atom after it absorbs all the energy of an incident photon. Excess energy (exceeding the binding energy) is given to the photoelectron as kinetic energy. If the emitted photoelectron was in an inner shell, a characteristic x-ray will be emitted as an outer shell electron replaces it. The probability (per atom) of a photoelectric absorption occurring σ_{pe} is proportional to :

$$\sigma_{\mathrm{pe}} \propto Z^3 E_\gamma{}^{-3} \tag{2.1}$$

For atomic number Z ≤15 and

$$\sigma_{\mathrm{pe}} \propto Z^{3.8} E_\gamma{}^{-3} \tag{2.2}$$

Where the atomic number Z≤15, where E_γ is the energy of the incident photon. The proportionality with $E_\gamma{}^{-3}$ means that Ionization due to the photoelectric effect is more likely at low energies(and is most common when E_γ is similar to E_{Shell} , the atomic binding energy) (P. Metcalfe, T. Kron, and P. Hoban,2007).

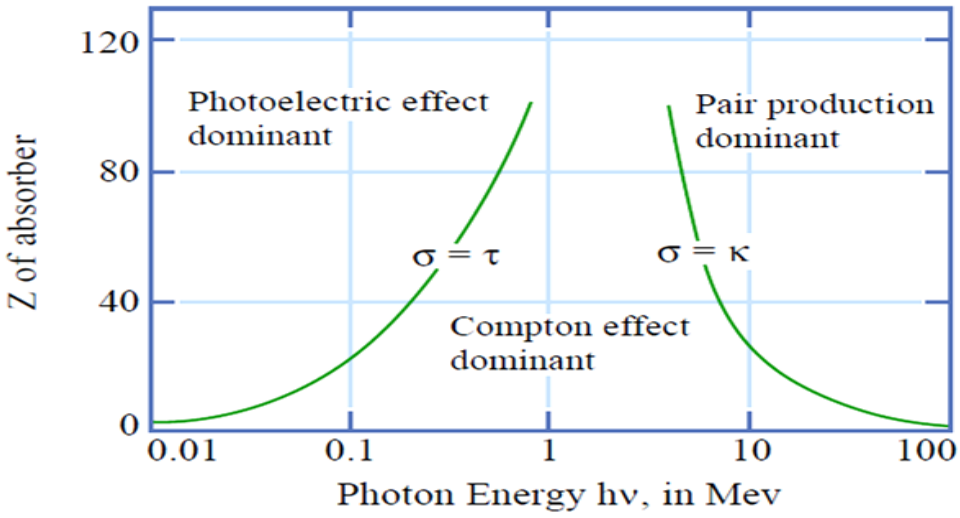

Figure 2.4 photon cross sections in water as a Function of photon energy.

Pair production can occur when a photon, with an energy greater than 1.022MeV, interacts with the electromagnetic field of a nucleus and produce an electron positionpair (those particles have rest mass energy of 0.511 MeV each, hence the E_{γ}=1.022MeV threshold) .

A related phenomenon is triple production, When a photon with an energy greater than 2.044 MeV, interacts with the electromagnetic field of an electron and produce an electron-positron pair and other electron. The combined probability of pair or triple production occurring σ_{pp} proportional to

$$\sigma_{\mathrm{pp}} \propto Z^2 \log E_{\gamma} \qquad (2.3)$$

This probability increases with increasing E_{γ}.The most likely interaction seen in *Figure 2.4* is Compton scattering. Compton scattering occurs when a recoil electron is emitted by an atom after it absorbs some of the energy of an incident photon in an inelastic collision(P. Metcalfe, T. Kron, and P. Hoban,2007).

The incident photon is then scattered at an angle related to the energy loss, such that conservation of momentum and mechanical energy can be maintained. The probability of Compton scattering, σ_{CO} is proportional to:

$$\sigma_{\mathrm{co}} \propto Z E_{\gamma}^{-\frac{1}{2}} \qquad (2.4)$$

Figures 2.3 and *2.4* indicate that for typical linear accelerator operation the electron production along the photon beam path is predominately achieved through Compton scattering. This interaction is not strongly dependent on atomic number, thus providing relatively uniform ionization as electron density doesn't vary too much over various tissues.

Indeed, Mayles mentions that "the mean free path (the distance between interactions) in bone is almost the same as that in water between 100 keV and 10 MeV after which pair production interactions become more prominent"(P. Mayles,et.al,2007)

.

2.3.2 Dosimetric Quantities:

The photons travel through the patient and ionize atoms and molecules, The imparted energy to the medium can be described as Energy imparted to the medium or energy transfer to the medium. There are three common dosimetric quantities *KERMA*, *CEMA*, And *Absorbed Dose*.

2.3.2.1 KERMA:

Kerma is an acronym for Kinetic Energy Released per unit Mass. It quantifies the average amount of energy transferred in a small volume from the indirectly ionizing radiation to directly ionizing radiation without concerns to what happens after this transfer.

The unit of kerma is joule per kilogram (J/kg)m And The name for the unit of kerma is the gray (Gy), where 1 Gy = 1 J/kg. Kerma is a quantity applicable to indirectly ionizing radiations, such as photons and neutrons.

$$\mathbf{K=\frac{\delta E}{\delta m}} \qquad (2.5)$$

Where δE in the equation above is the transferred energy and δm is the mass.

The particles ejected in these ionization events will travel some distance from the interaction site, in the case of electrons it can be several centimeters , depending on the density of the medium (which may not be uniform), in a direction determined during the interaction.

The energy transferred to electrons by photons can be expended in two distinct ways: first through the collision interactions (soft collisions and hard collisions), secondthrough the radiative interactions (bremsstrahlung and electron–positron annihilation). The total kerma is therefore usually divided into two components: the collision kerma K_{col} and the radiative kerma K_{rad}.

2.3.2.2 CEMA:

Similar to kerma, cema is an acronym for Converted Energy per unit MAss. It quantifies the average amount of energy converted in a small volume from directly ionizing radiations such as electrons and protons in collisions with atomic electrons without concerns to what happens after this transfer.

$$\mathbf{C=\frac{\delta \bar{\epsilon} c}{\delta m}} \qquad (2.6)$$

Where $\delta\bar{\epsilon}c$is the average amount of energy converted, δm the volume mass. The unit of cema is the same unit of the Kerma ingray (Gy).

Cema differs from kerma in that Cema involves the energy lost in electronic collisions by the incoming charged particles, and Kerma involves the energy imparted to outgoing charged particles.

2.3.2.3 Absorbed Dose:

Absorbed dose is a quantity applicable to both indirectly and directly ionizing radiations. Indirectly ionizing radiation means that the energy is imparted to matter in a two-step process, In the first step (resulting in kerma), the indirectly ionizing radiation transfers energy as kinetic energy to secondary charged particles. In the second step, these charged particles transfer a major part of their kinetic energy to the medium (finally resulting in absorbed dose). In the other hand, directly ionizing radiation means that the charged particles transfer a major part of their kinetic energy directly to the medium (resulting in absorbed dose).

The measure of energy deposition (as opposed to transfer or release) is known as dose, or more specifically ‘absorbed dose’, expressed with the unit Gray (Gy) where:

$$1\text{Gy} = 1\frac{\text{J}}{Kg} \qquad (2.7)$$

The absorbed dose can be described by the following equation :

$$D = \frac{\delta \bar{\epsilon}}{\delta m} \qquad (2.8)$$

Where $\delta\bar{\epsilon}$ represents the net energy imparted to a volume and δm the volume mass. The net energy imparted can be more explicitly defined as :

$$\delta\bar{\epsilon} = R_{in} - R_{out} + \sum Q \qquad (2.9)$$

Where R_{in} is the sum of the energies entering the volume (excluding rest mass energy), R_{out} is the sum of the energies that exit the volume (excluding rest mass energy) and$\sum$ Q is the sum of any mass conversion (or change in rest mass energy) (P. Mayles,et.al,2007).

When the net sum of the energies associated with charged particles is zero, that is, when the charged particle energy in is equal to the charged particle energy out, then charged particle equilibrium is said to exist.

The mean free path for Compton scattering does not change significantly between different media. It does however vary with the photon energy, the attenuation of the beam through the patient results in a change in the energy spectrum; and that changes the probability with which interactions occur. This results in the production of a nonlinear depth-dose profile. *Figure 2.5* presents dose deposition measurements against water depth for a 10 MV photon beam.

The largest dose deposition occurs between 1 and 2 cm, which called maximum dose (D_{max}) depth. It does not occur at the surface because charged particle equilibrium does not exist there, more charged particles are leaving the region than entering it. This region between the surface and the maximum dose depth is known as the electron buildup region (KHAN, F.M.,2003).

2.4 Cavity Theory:

In order to measure the absorbed dose in a medium, it is necessary to introduce a radiation sensitive device (dosimeter) into the medium. Generally, the sensitive medium of the dosimeter will not be of the same material as the medium in which it is embedded. Cavity theory relates the absorbed dose in the dosimeter's sensitive medium (cavity) to the absorbed dose in the surrounding medium containing the cavity.

Cavity sizes are referred to as small, intermediate or large in comparison with the ranges of secondary charged particles produced by photons in the cavity medium. If, for example, the range of charged particles (electrons) is much larger than the cavity dimensions, the cavity is regarded as small.

Various cavity theories for photon beams have been developed, which depend on the size of the cavity; for example, the Bragg– Gray and Spencer–Attix theories for the small cavities and the Burlin theory for cavities of intermediate sizes.

2.4.1 Bragg–Gray cavity theory

The Bragg–Gray cavity theory was the first cavity theory developed to provide a relation between the absorbed dose in a dosimeter and the absorbed dose in the medium containing the dosimeter. The conditions for application of the Bragg–Gray cavity theory are:

- The cavity must be small when compared with the range of charged particles incident on it, so that its presence does not perturb the fluence of charged particles in the medium.
- The absorbed dose in the cavity is deposited solely by charged particles crossing it (i.e. photon interactions in the cavity are assumed negligible and thus ignored).

The result of the first condition is that the electron fluencies in are the same and equal to the equilibrium fluence established in the surrounding medium. This condition can only be valid in regions of CPE or TCPE. In addition, the presence of a cavity always causes some degree of fluence perturbation that requires the introduction of a fluence perturbation correction factor.

The second condition implies that all electrons depositing the dose inside the cavity are produced outside the cavity and completely cross the cavity. No secondary electrons are therefore produced inside the cavity and no electrons stop within the cavity.

Under these two conditions, according to the Bragg–Gray cavity theory, the dose to the medium D_{med} is related to the dose in the cavity D_{cav} as follows:

$$D_{med} = D_{cav}\left(\frac{\bar{S}}{\rho}\right)_{med,cav} \qquad (2.9)$$

Where $(\bar{S}/\rho)_{med,\,cav}$ is the ratio of the average unrestricted mass collision stopping powers of the medium and the cavity.

The use of unrestricted stopping powers rules out the production of secondary charged particles (or delta electrons) in the cavity and the medium. Although the cavity size is not explicitly taken into account in the Bragg– Gray cavity theory, the fulfillment of the two Bragg–Gray conditions will depend on the cavity size, which is based on the range of the electrons in the cavity medium, the cavity medium and the electron energy. A cavity that qualifies as a Bragg–Gray cavity for high energy photon beams, for example, may not behave as a Bragg–Gray cavity in a medium energy or low energy X-ray beam. A dosimeter can be defined generally as any device that is capable of providing a reading that is a measure of the average absorbed dose deposited in its sensitive volume by ionizing radiation. A dosimeter can generally be considered as consisting of a sensitive volume filled with a given medium, surrounded by a wall of another medium. In the context of cavity theories, the sensitive volume of the dosimeter can be identified as the ‘cavity’, which may contain a gaseous, liquid or solid medium. Gas is often used as the sensitive medium, since it allows a relatively simple electrical means for collection of charges released in the sensitive medium by radiation. The medium surrounding the cavity of an ionization chamber depends on the situation in which the device is used.

In an older approach, the wall (often supplemented with a buildup cap) serves as the buildup medium and the Bragg–Gray theory provides a relation between the dose in the gas and the dose in the wall. This is referred to as a thick walled ionization chamber and forms the basis of cavity chamber based air kerma in-air standards.

If, however, the chamber is used in a phantom without a buildup material, since typical wall thicknesses are much thinner than the range of the secondary electrons, the proportion of the cavity dose due to electrons generated in the phantom greatly exceeds the dose contribution from the wall, and hence the phantom medium serves as the medium and the wall is treated as a perturbation to this concept.

In the case of a thick walled ionization chamber in a high energy photon beam, the wall thickness must be greater than the range of secondary electrons in the wall material to ensure that the electrons that cross the cavity arise in the wall and not in the medium. The Bragg–Gray cavity equation then relates the dose in the cavity to the dose in the wall of the chamber. The dose in the medium is related to the dose in the wall by means of a ratio of the mass– energy absorption coefficients of the medium and the walls, by assuming that:

- The absorbed dose is the same as the collision kerma.
- The photon fluence is not perturbed by the presence of the chamber.

The dose to the cavity gas is related to the ionization produced in the cavity as follows:

$$D_{\text{gas}} = \frac{Q}{m}\left(\frac{\overline{W}_{\text{gas}}}{e}\right) \qquad (2.10)$$

Where Q is the charge (of either sign) produced in the cavity and m is the mass of the gas in the cavity. In the case of a thin walled ionization chamber in a high energy photon or electron beam, the wall cavity and central electrode are treated as

$$D_{\text{med}} = \frac{Q}{m}\left(\frac{\overline{W}_{\text{gas}}}{e}\right) s_{\text{med,gas}} p_{\text{fl}}\, p_{\text{dis}}\, p_{\text{wall}}\, p_{\text{cel}} \qquad (2.11)$$

Where P_{fl} is the electron fluence perturbation correction factor; P_{dis} is the correction factor for displacement of the effective measurement point; P_{wall} is the wall correction factor; P_{cel} is the correction factor for the central electrode.Values for these multiplicative correction factors are summarized for photon and electron beams in typical dosimetry protocols such (IAEA TRS 398).

2.4.1.1 Stopping power ratios

Although cavity theory was designed to calculate ratios of absorbed doses, the practical application of the Spencer–Attix cavity theory has always required additional correction factors. Since the central component of the Spencer–Attix cavity theory results in averaging stopping powers, Spencer– Attix dose ratios are often referred to as 'stopping power ratios'. In photon beams, except at or near the surface, average restricted stopping power ratios of water to air do not vary significantly as a function of depth.

Stopping power ratios (with D = 10 keV) under full buildup conditions are shown in *Table 2.1*. Stopping power ratios not only play a role in the absolute measurement of absorbed dose, they are also relevant in performing accurate relative measurements of absorbed dose in regimes in which the energy of the secondary electrons changes significantly from one point in a phantom to another.An important example of this is apparent from Fig. 2.5, which shows restricted stopping power ratios (D = 10 keV) of water to air for electron beams as a function of depth in water.

Table 2.1: Average restricted stopping power ratio of water to the air, $S_{water,\ air}$, for different photon spectra in the range from ^{60}Co γrays to 35 MV X rays:

Photon Spectrum	$S_{water,air}$
^{60}Co	1.134
4MV	1.131
6 MV	1.127
8 MV	1.121
10 MV	1.117
15 MV	1.106
20 MV	1.096
25 MV	1.093
35 MV	1.084

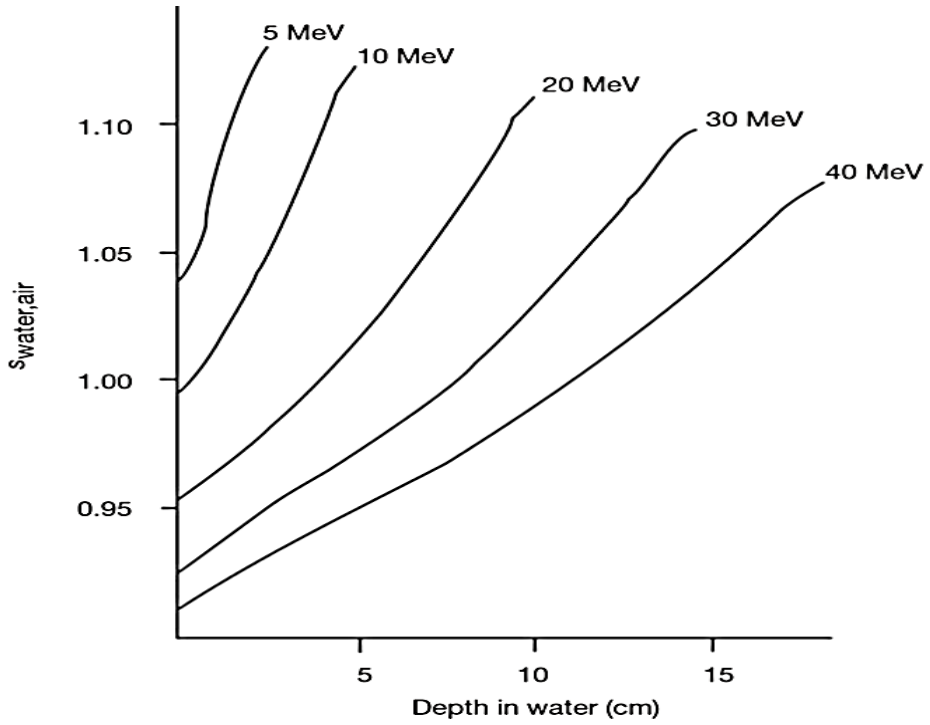

Figure 2.5: Restricted collision stopping power water to air ratio (D = 10 keV) as a function of depth for different monoenergetic electron energies.

Note that these curves are for monoenergetic electrons; protocols or codes of practice for electron dosimetry provide fits of stopping power ratios for realistic accelerator beams.However, *Figure2.5* shows clearly that the accurate measurement of electron beam depth dose curves requires depth dependent correction factors (KHAN, F.M,2002).

2.5 Ionization chamber dosimetry systems:

A radiation dosimeter is a device, instrument or system that measures or evaluates, either directly or indirectly, the quantities exposure, kerma, absorbed dose or equivalent dose, or their time derivatives (rates), or related quantities of ionizing radiation. A dosimeter along with its reader is referred to as a dosimetry system. Measurement of a dosimetric quantity is the process of finding the value of the quantity experimentally using dosimetry systems. The result of a measurement is the value of a dosimetric quantity expressed as the product of a numerical value and an appropriate unit. (KHAN, F.M.,2003)

To function as a radiation dosimeter, the dosimeter must possess at least one physical property that is a function of the measured dosimetric quantity and that can be used for radiation dosimetry with proper calibration. In order to be useful, radiation dosimeters must exhibit several desirable characteristics. For example, in radiotherapy exact knowledge of both the absorbed dose to water at a specified point and its spatial distribution are of importance, as well as the possibility of deriving the dose to an organ of interest in the patient. In this context, the desirable dosimeter properties will be characterized by accuracy and precision, linearity, dose or dose rate dependence, energy response, directional dependence and spatial resolution. Obviously, not all dosimeters can satisfy all characteristics.

Ionization chambers are used in radiotherapy and in diagnostic radiology for the determination of radiation dose. The dose determination in reference irradiation conditions is also called beam calibration. Ionization chambers come in various shapes and sizes, depending upon the specific requirements, but generally they all have the following properties:

- An ionization chamber is basically a gas filled cavity surrounded by a conductive outer wall and having a central collecting electrode (Figure 2.6). The wall and the collecting electrode are separated with a high quality insulator to reduce the leakage current when a polarizing voltage is applied to the chamber.
- A guard electrode is usually provided in the chamber to further reduce chamber leakage. The guard electrode intercepts the leakage current and allows it to flow to ground, bypassing the collecting electrode. It also ensures improved field uniformity in the active or sensitive volume of the chamber, with resulting advantages in charge collection.
- Measurements with open air ionization chambers require temperature and pressure correction to account for the change in the mass of air in the chamber volume, which changes with the ambient temperature and pressure.

Electrometers are devices for measuring small currents, of the order of 10–9 A or less. An electrometer used in conjunction with an ionization chamber is a high gain, negative feedback, operational amplifier with a standard resistor or a standard capacitor in the feedback path to measure the chamber current or charge collected over a fixed time interval, as shown schematically in Figure 2.6 bellow.

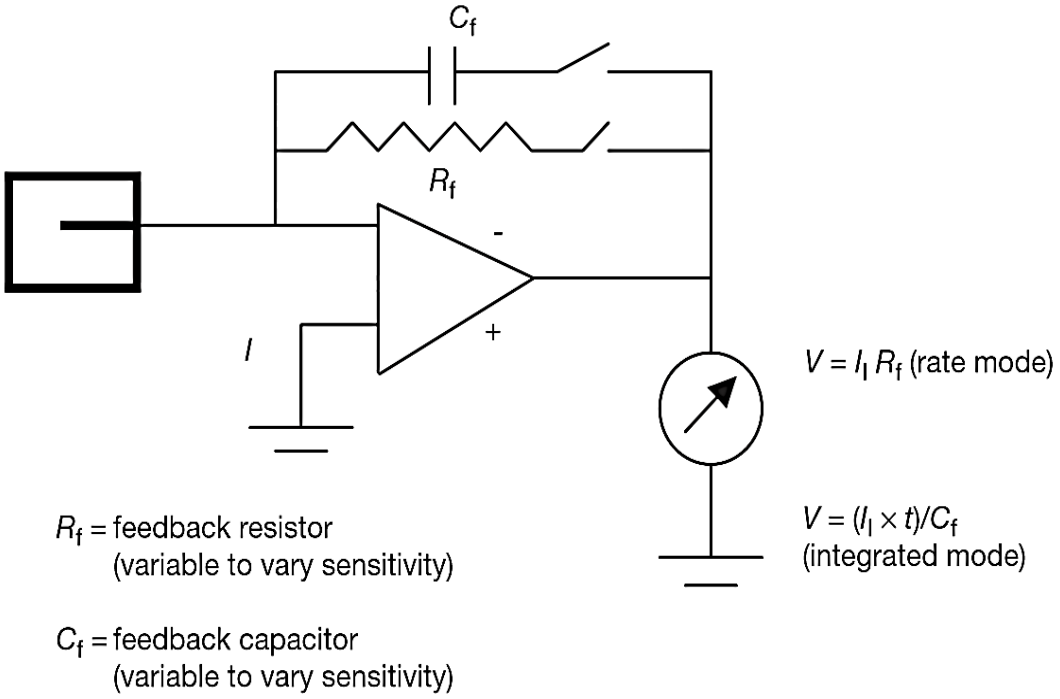

Figure2.6: Electrometer in feedback mode of operation.

2.5.1 Cylindrical ionization chambers:

The most popular cylindrical ionization chamber is the 0.6 cm3 chamber designed by Farmer and originally manufactured by Baldwin, but now available from several vendors, for beam calibration in radiotherapy dosimetry. Its chamber sensitive volume resembles a thimble, and hence the Farmer type chamber is also known as a thimble chamber. A schematic diagram of a Farmer type thimble ionization chamber is shown in *Figure 2.7*.

Cylindrical chambers are produced by various manufacturers, with active volumes between 0.1 and 1 cm3. They typically have an internal length no greater than 25 mm and an internal diameter no greater than 7 mm. The wall material is of low atomic number Z (i.e. tissue or air equivalent), with the thickness less than 0.1 g/cm2. A chamber is equipped with a buildup cap with a thickness of about 0.5 g/cm2 for calibration free in air using ^{60}Co radiation. The chamber construction should be as homogeneous as possible, although an aluminum central electrode of about 1 mm in diameter is typically used to ensure flat energy dependence. Construction details of various commercially available cylindrical chambers are given in the IAEA Technical Reports Series (TRS 277) and (TRS 398) codes of practice.

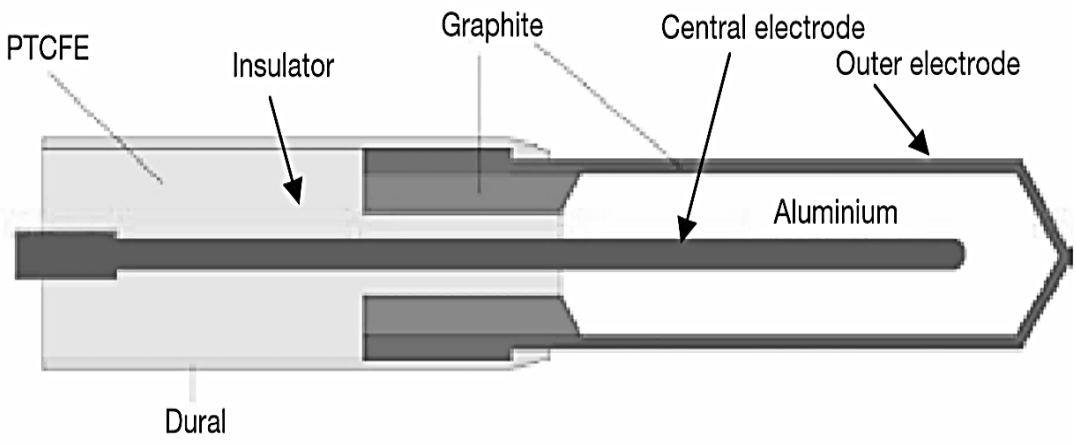

Figure2.7: Basic design of a cylindrical Farmer type ionization chamber.

2.5.2 Parallel-plate ionization chambers:

A parallel-plate ionization chamber consists of two plane walls, one serving as an entry window and polarizing electrode and the other as the back wall and collecting electrode, as well as a guard ring system. The back wall is usually a block of conducting plastic or a non-conducting material (usually Perspex or polystyrene) with a thin conducting layer of graphite forming the collecting electrode and the guard ring system on top. A schematic diagram of a parallel-plate ionization chamber is shown in *Figure 2.8*the parallel-plate chamber is recommended for dosimetry of electron beams with energies below 10 MeV.

It is also used for surface dose and depth dose measurements in the buildup region of megavoltage photon beams. The characteristics of commercially available parallel-plate chambers and the use of these chambers in electron beam dosimetry are explained in detail in the TRS 381 and TRS 398 codes of practice. Some parallel-plate chambers require significant fluence perturbation correction because they are provided with an inadequate guard width.

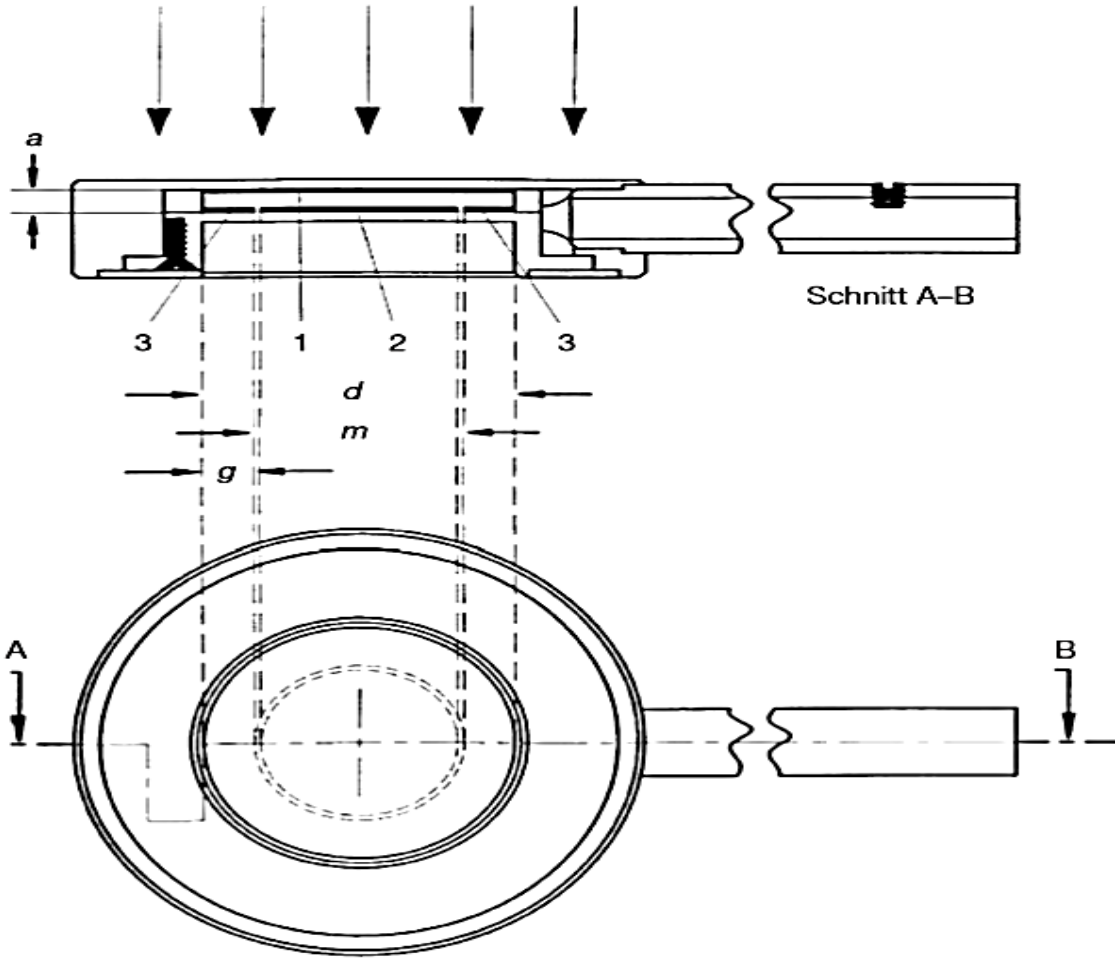

Figure 2.8: Parallel-plate ionization chamber. 1: the polarizing electrode. 2: the measuring electrode. 3: the guard ring. a: the height (electrode separation) of the air cavity. d: the diameter of the polarizing electrode. m: the diameter of the collecting electrode. g: the width of the guard ring.

2.6 Determination of the absorbed Dose to water:

It is assumed that the ionization chamber or a dosimeter with a calibration factor $N_{D,\,w,\,Qo}$ in terms of absorbed dose to water at a reference quality Q_o. The chamber is positioned according to the reference conditions and the absorbed dose to water is given by:

$$D_{w,Q} = M_Q N_{D,\,w,\,Qo} k_{Qo} \qquad (2.12)$$

Where M_Q is the reading of the dosimeter and $k_{Q,\,Qo}$ is the correction factor which corrects for the difference between the reference beam quality Q_o and the actual quality Q being used. This equation is valid for all the radiation fields for which this Code of Practice applies. Details on the reference conditions to be used for radiotherapy beam calibrations and values for the factor $k_{Q,Qo}$.

Recommendations on relative dosimetry, namely the determination of distributions of absorbed dose, are mentioned with more details in IAEA TRS.398. Although the correction factor $k_{Q,Qo}$is not different in kind from all other correction factors for influence quantities, because of its dominant role it is treated separately in each section in the IAEA TRS.398.

2.6.1 Reference Condition of measurement:

The reference conditions for determination of absorbed dose to water are given in *Table 2.2.* The determination of absorbed dose under reference conditions and its generalformalism is shown in equation (2.12) (KHAN, F.M.,2003).

.From *table 2.2* the field size is defined at the plane of the reference point of the detector, placed at the recommended depths in the water phantom.

In an ESTRO-IAEA report on Monitor Unit calculations, the use of a single reference depth Z_{ref} = 10 g cm-^{2} for all photon beam energies is recommended. However, maybe we prefer to use the same reference depth as that used for ^{60}Co beams, i.e. Z_{ref} = 5 g cm^{-2}; this option is therefore allowed in this Code of Practice.

If the reference dose has to be determined for an isocentric set up, the Source Axial Distant (SAD) of the accelerator shall be used even if this is not 100 cm. The field size is defined at the surface of the phantom for a SSD type setup, whereas for a SAD type set-up it is defined at the plane of the detector placed at the reference depth in the water phantom at the isocenter of the machine.

Table2.2: Reference conditions for the determination of the photon beam Quality ($TPR_{20,10}$):

Influence quantity	Reference value or reference characteristics
Phantom material	Water
Chamber type	Cylindrical or plane parallel
Measurement depth	z_{ref} for $TPR_{20,10} < 0.7$, 10 g cm^{-2} (or 5 g cm^{-2}) for $TPR_{20,10} \geq 0.7$, 10 g cm^{-2}
Reference point of chamber	For cylindrical chambers, on the central axis at the Centre of the cavity volume. For plane-parallel chambers, on the inner surface of the window at its center.
Position of reference point of the chamber	For cylindrical and plane-parallel chambers, at the measurement depths
SSD/SCD	100 cm
Field size	10 cm x 10 cm

2.7 Absolute and Relative dosimetry:

A direct measure of ionization or absorbed dose under standard conditions is the Absolute Dosimetry, which are things like calorimetry, electrons released, or ion formation where the number of valence changes in a known amount of ions is directly related to the number of electrons. Itrequired for every radiation quality once, The Determination of absorbed dose (Gy) at one reference point in a phantom.

It must be in Well-defined geometry (example for a linear accelerator: measurements in water, at 100cm FSD, 10x10cm^2 field size, depth 10cm. the most important thing is Follows the common international protocols for example(DIN 6800, AAPM TG-51,and IAEA TRS 398). If the absolute dosimetryis incorrect everything will be wrong.

In the other hand, the relative Dosimetry is relates the dose under non-reference conditions to the dose under reference conditions. Typically at least two measurements are required the first one in conditions where the dose shall be determined and the other one in conditions where the dose is known. The relative dosimetry is refers to the use of a dosimeter which has a secondary standard, This dose is actually 'measured' by a reference dosimeter, Examples for relative dosimetry is Characterization of a radiation beam percentage depth dose, tissue maximum ratios or similar, profiles,and Determination of factors affecting output like the field size factors, applicator factors, filter factors, wedge factors, and patient specific factors (*e.g.* electron cut-out).

2.8 Descriptors of photon beam Dose Distribution:

Photon beams may be represented as a depth dose chart (along the central beam axis), a beam profile (perpendicular to the beam axis), or an isodose chart (a plane parallel or perpendicular to the beam axis).

2.8.1 Percent Depth Dose :

A chart showing dose along the central beam axis is known as a depth dose distribution. Dose is normalized to the point of maximum dose, z_{max}. The PDD is dependent on beam energy, field size, and source-surface distance and is also affected by inhomogeneities.If we take the photon energy of 6 MV Depth Dose Chart ; most electrons liberated by 6 MV photons will have an energy of around 1- 2 MeV, but this varies from close to zero up to the maximum energy of the photon.

Electrons with this energy will travel around 1 cm, explaining the buildup region of this photon beam. Once the depth of maximum dose reached 1. 6 cm, the dose falls off gradually to 90% by 4 cm. It then continues to fall by about 10 % every 2.5 cm, the rate of dose fall off slowing after 9 cm.

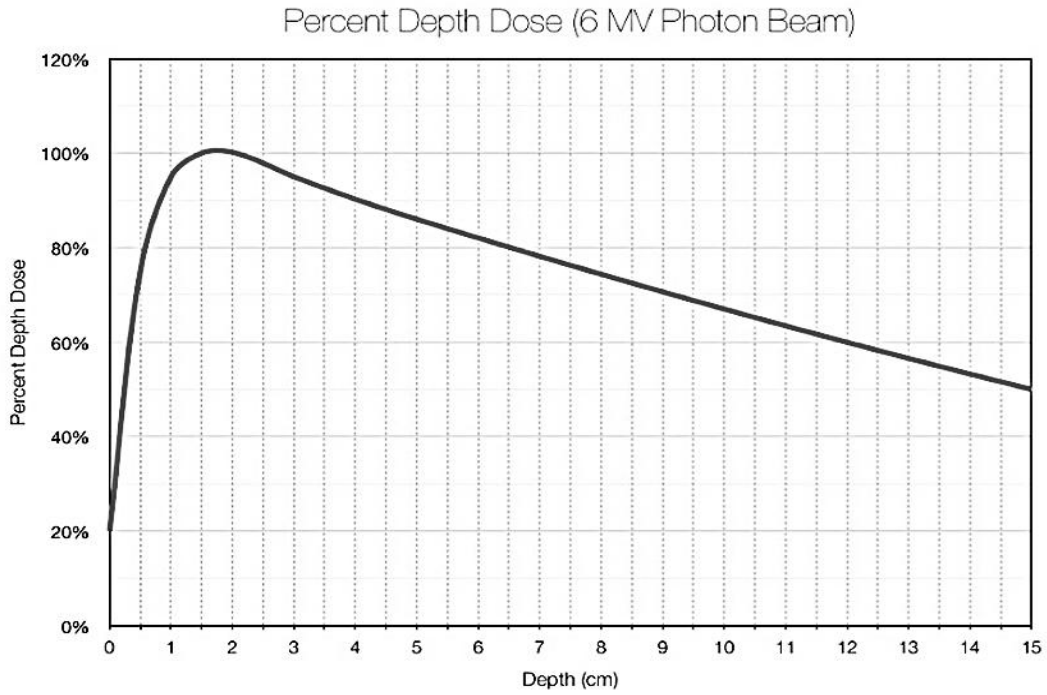

Figure 2.9: 6 MV depth dose chart, 10 x 10 field size, 100 cm SSD.

2.8.2 Beam Profile:

The variation of dose occurring on a line perpendicular to the central beam axis at a certain depth is known as the beam profile. It represents how dose is altered at points away from the central beam axis. There are typically three parts:

- The central region which is usually flat and includes doses over 80% of the central beam axis.
- The penumbra region where dose falls off rapidly at the beam edge, between the doses of 20-80% of the central beam axis.
- The umbra region where dose is minimal (under 20% of the central beam dose).

Other distinctive features are the lateral horns, which are only present in photon beams (and more pronounced for 18 MV photons). The lateral horns are caused by the flattening filter, which aims for a flat dose at a particular depth. To create this, at depths above this point the beam has 'horns' of higher dose. (KHAN, F.M.,2003)

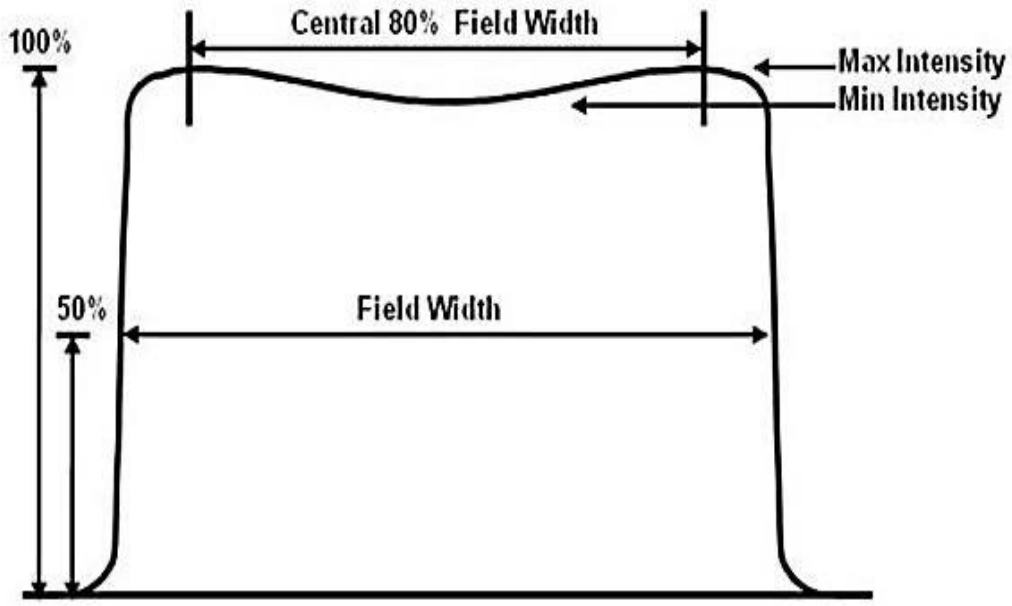

Figure 2.10: Photon beam profile.

2.8.3 Isodose Chart:

Isodose charts are two dimensional representations of dose distribution. They are formed by lines drawn along equal increments of percent dose, relative to a particular point.

- For constant SSD techniques, '100% dose' is taken as the depth of dose maximum on the central axis for a beam.
- For constant SAD (isocentric) techniques, '100% dose' is the dose at the isocenter of the machine.

Isodose charts represent a combination of the percent depth dose and the beam profile at multiple points along the central axis. Features such as zmax and the penumbra are visible. Most commonly, isodose charts are drawn on a plane parallel to the beam direction, but they may also be drawn on a plane perpendicular to the central axis.

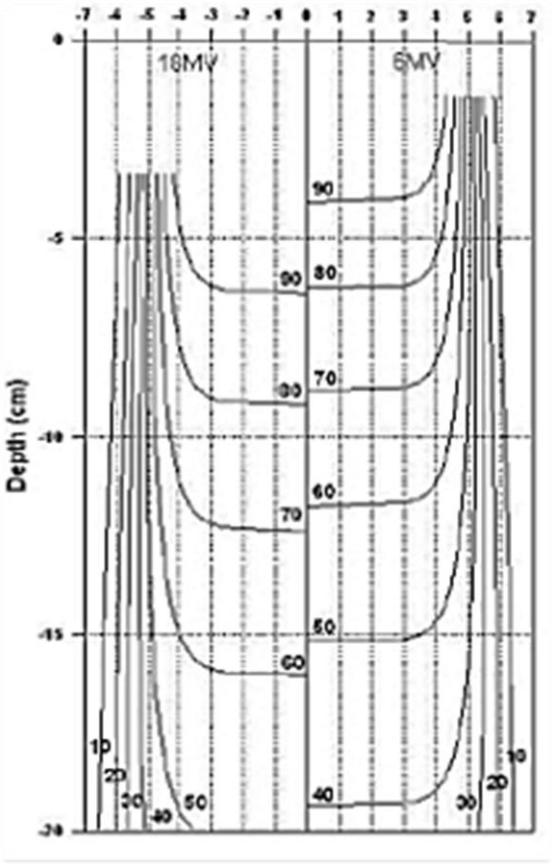

Figure 2.11:Isodose chart. SSD type, 6, 16 MV Photon beam, SSD =100 cm, field size of 10 × 10 cm.

2.9 Components of Dose Distribution:

- **Surface Dose:**

The entrance dose is the dose at the point where the beam intersects the patient or phantom. Kilovoltage x-rays have an entrance dose of 100% as they fall off rapidly thereafter.

The surface dose of megavoltage x-rays reduces as beam energy increases and can be as little as 10-20% of Zmax. Surface dose is due to a combination of primary radiation, scatter from the collimators and air, and backscatter from the treated volume.

- **Exit Dose:**

The exit dose is the dose at the point where the beam exits the patient. It shows a rapid fall off in absorbed dose due to lack of scatter from distant parts of the beam.

- **Skin Sparing:**

Skin sparing is a phenomenon seen with megavoltage photon beams only. It is due to decreased entrance dose for these beams.

The skin receives reduced dose than deeper seated tissues due to this. Skin sparing is one of the reasons for using megavoltage beams.

- **Beam Flatness:**

Beam Flatness refers to variation in the beam strength across the central part of the beam. Within the central region, ratio of the dose over 90% to that under 90% is known as the uniformity index.

The ICRU recommends that the uniformity index is kept above a value dependent on beam quality and field size. Dose in the central region should also be kept beneath 103% of the central axis dose.

- **Beam Symmetry:**

Beam Symmetry refers to the ratio of dose at a pair of points located opposite each other from the central beam axis. The AAPM recommends that the dose at these two points should vary by less than 2%.

- **Penumbra:**

The penumbra is the region of rapid dose falloff located at the edge of a beam. It is usually considered to be the part of the dose that lies between 20% and 80% of the central axis dose. The penumbra is formed by three components:

-The geometric penumbra is due to a finite source size. It is more of a concern in teletherapy machines where the source is between 1 and 2 cm in size.

-The transmission penumbra is due to transmission of photons through the primary, secondary or tertiary collimators.

1. -The physical penumbra is due a combination of the geometric penumbra, transmission penumbra and electron scattering at the beam edges. (KHAN, F.M.,2003)

2.10 Radiobiology:

There are two processes by which tissue is damaged by ionizing radiation: the direct ionization of DNA and, more prominently (in traditional therapies) [30], the indirect damage through the creation of free radicals in intracellular material. Direct ionization is the most effective mechanism for damage, forming radical cations which lead to DNA strand breaks [31].

The indirect effect of radiation involves the production of free radicals, predominately hydroxyl, in the intracellular volume (largely comprised of water). Electrons ionize the H_20 molecules:

$$H_20 \rightarrow H_2O^+ + e^- \qquad (2.13)$$

And then hydroxyl ($\bullet OH$) is subsequently formed:

$$H_2O^+ + H_20 \rightarrow \bullet OH + H_3O^+ \qquad (2.14)$$

The hydroxyl radical can cause strand breaks by creating a radiochemical lesion when it diffuses into a DNA molecule. This will only occur when the radical is produced within approximately 10-8 meters of the DNA molecule (P. Metcalfe, T. Kron, and P. Hoban,2007)

. Hall and Giaccia suggest that two thirds of x-ray damage to DNA in mammalian cells is caused by the hydroxyl radical (E. J. Hall and A. J. Giaccia,2006).

Absorbed dose is the standard physical measure used to predict the effect of an exposure to radiation, the biological response also depends on the radiation type and the tissue exposed. Radiation with a high linear energy transfer (LET) is more likely to cause direct damage.

Still, it is possible to make generalizations regarding cellular response to external beam photon therapy: the median lethal dose values (level of absorbed dose that would result in 50% of total cells losing reproductive capacity) for malignancies are typically around 2 Gy ,(M. Tubiana,et.al,1990)

. According to Myles, a typical tumor (weighing tens or hundreds of grams) might contain 10^9congenic cells (potentially as few as 1% of the total cells).

A simple substitution suggests it would take approximately 30 deliveries of 2 Gy to effectively 'remove' congenic cells, resulting in a total of 60 Gy absorbed dose (ignoring repopulation and other biological factors).

The dose delivered in a clinical treatment will generally fall between 20 to 80 Gy total. Each delivery is referred to as a 'fraction', and the multiple fractions are typically delivered daily over the course of a few weeks. Fractionation is motivated by a number of radiobiological variables: it helps spare normal tissue through repair and repopulation, and increases tumor cell death via cell cycle synchronization and oxygenation.

The concentration of molecular oxygen in tissue has an effect on the impact of indirect damage. It is suggested by Molls et al (M. Molls,1998) that the free radicals produced by radiation are fixed in the presence of oxygen, which decreases the likelihood of cellular repair. This means that in low oxygen (hypoxic) cells such as in tumors, where the blood supply is poor, the likelihood of indirect damage is decreased. This is one of the reasons a radiotherapy treatment is fractionated to allow oxygenation of the tumor cells between dose deliveries.

Bergonie and Tribondeaus' Law states that radiation sensitivity is increased when cells are actively proliferating at the time of the exposure. Furthermore, excessive proliferation results in poor cellular differentiation, so cancer cells are both more susceptible to damage and less able to repair it. This is another motivation for dose fractionation: to allow healthy cells to repair damage.

Since radiation does not significantly discriminate between healthy and cancerous cells, the potential consequences of exposure need to be considered. Swelling of soft tissue, ulcerations in mucous linings and hair loss may be deemed acceptable side effects.

Similar swelling in critical organs might pose serious quality of life concerns or mortality risks. Necrosis can result from excessive levels of radiation in tissue. Long-term concerns can include infertility and the development of radiation- induced malignancies.

The goal of radiotherapy is to deliver the greatest therapeutic benefit: minimizing complications in healthy tissue while maximizing the damage, or control, of the tumor. Achieving this requires not only an accurate prediction of dose deposition, but also an understanding of how tissue responds to radiation.

The mean lethal dose is the amount of absorbed energy that results in 50% of the exposed cells being killed. The rate at which cells are killed on subsequent exposures drops off exponentially: an exposure of 2 x the mean lethal dose would kill 75% of the exposed cells. The surviving fraction (SF) of cells following an exposure to dose D can be defined as :

$$SF(D) = \frac{K}{K_o} \exp(-\alpha D) \qquad (2.15)$$

Where k is the number of cells left alive, k_o is the initial number of cells and is a constant of proportionality indicating radio sensitivity. This approach is simplistic: it is derived from "single-target theory" (P. Metcalfe, T. Kron, and P. Hoban,2007); where the SF is defined as

$$SF(D) = \exp\left(-\frac{D}{D_o}\right) \qquad (2.16)$$

Where D_o describes the radioresistance of irradiated cells and is called the mean (not median) lethal dose (A. Niemierko,1997).

This does not however match experimental cell survival curves because it does not consider cellular repair, the effect of multiple strand breaks, the relation of these two variables to dose rate, the delivery of doses in fractions, and the periodicity of these deliveries and so on. This is the motivation for radiobiological modelling: to translate dose to more biologically relevant quantities (P. Metcalfe, T. Kron, and P. Hoban,2007)

.This modeling begins with the linear quadratic model, where, for a single delivery of dose D, the cell survival curve is defined as:

$$SF(D) = \exp(-D(\alpha+\beta D)) \qquad (2.17)$$

Where α and β are linear and quadratic coefficients respectively, characteristic for a given type of tissue and often presented as a α/β ratio (P. Metcalfe, T. Kron, and P. Hoban,2007).

These values are obtained via experimentation: cell colonies are seeded, irradiated, allowed to repair and then counted. The α/β ratios for tumors are typically higher than those of normal tissues, due to the faster rate of cell division.

Typical ratios are 3 for normal tissue and 10 for tumors, though prostate cancer differs significantly in having a lower α/β ratio, with estimations varying between 1.5 Gy and 3.1 to 3.9 Gy (H. B. Kal, and M. P., van Gellekom,2003) In all cases α exceeds β.

The survival rate for a treatment split into *n*-fractions of dose D can be most simply expressed as

$$SF(n, D) = SF(D)^{n} \quad (2.18)$$

And so the linear quadratic model becomes, by substitution,

$$SF(n, D) = \exp(-nD(\alpha+\beta D)) \quad (2.19)$$

A motivation behind dose fractionation can be observed here: for late-responding normal tissue (which has a low α/β ratio), cell survival drops off more quickly for high doses (as the quadratic term dominates). When dose values are kept smaller, the linear term dominates, and this is generally higher for malignant tissue.

The best therapeutic ratio can thus be obtained with small dose fractions. The linear quadratic model can be expanded to predict fractionation effects [38]

$$SF(n, D, T) = \exp(-n D(\alpha + \beta D) - \gamma T) \quad (2.20)$$

Where T is the overall treatment time and γ is a parameter reflecting repopulation between deliveries, defined as

$$\gamma = \ln(2/T_{pot}) \quad (2.21)$$

Here T_{pot} is the potential doubling time, the time required for the number of cells to double.

The linear quadratic model allows us to quantify cellular survival fractions in terms of dose deposition: which is one step closer to quantifying the tumor control probability (TCP) and the normal tissue complication probabilities (NTCP), by using the "critical volume model" [39]. These concepts require an understanding of tissue organization: tissue can be described as consisting of functional sub-units (FSUs) (A. Niemierko and M. Goitein,1993), which are inactive if all cells within it are killed. For a given organ (or tumor) we can define a complication as occurring when a given number of FSUs are made inactive.

For a tumor, the presence of an active FSU, which might be the result of a treatment which did not uniformly irradiate the tumor, increases the risk of recurrence (P. Metcalfe, T. Kron, and P. Hoban,2007), as an FSU is defined here as the volume that one congenic cell could repopulate (A. Niemierko and M. Goitein,1993)

Tumors are thus referred to as having parallel architecture: the probability of tumor control is strictly dependent on the number of FSUs killed, that is, control of the tumor requires all FSUs to be terminated. The probability of killing an FSU, PFSU, can be defined as (A. Niemierko and M. Goitein,1993).

$$P_{FSU}(n, D) = (1 - SF(n, D))^{k} = (1 - e^{(-n D(\alpha + \beta D))})^{k} \quad (2.22)$$

Where k is the number of cells per FSU, which in the case of a tumor would equal the product of ρ (the clonogen density), and V the volume (ATTIX, F.H.,1986). The probability of killing M FSUs of a total N can be derived as (A. Niemierko and M. Goitein,1993)

$$PM = \sum_{i=M+1}^{n} (n/i)\, P_{FSU}^{i} (1 - P_{FSU})^{(N-i)} \quad (2.23)$$

In the case of a tumor$M=N$ and P_N is referred to as the tumor control probability. For normal tissue P_M is known as the normal tissue complication probability and M varies depending on 'tissue architecture'. In organs with a parallel architecture, such as the kidney, where the inactivation of some nephrons will not necessarily result in a complication, M might be similar to N. In organs with a serial structure, such as the spinal cord, where the death of a small percentage of *FSUs* might have serious repercussions, M is quite small.

The *TCPs* and *NTCPs* discussed give some insight to what magnitude of dose might be desirable when designing a therapeutic strategy: the dose prescribed for the tumour is based on the size and stage of progression (related to the number of clonogenic cells) in order to give the greatest chance of tumour control, while tolerance doses can be defined for the organs at risk based on complication probabilities.

Calculated *TCP* and *NTCP* values can be combined in two ways: as an uncomplicated tumor control probability (*UTCP*), which is equal to

$$\text{UTCP} = \text{TCP}\,(1 - \text{NTCP}) \tag{2.24}$$

As a therapeutic ratio, ratios of doses for which the NTCP and TCP functions are equal (a measure of maximal displacement between the two functions):

$$\text{TR} = \left\{ D \,|\, \forall x : \frac{NTCP(x)}{TCP(x)} \leq \frac{NTCP\,(D)}{TCP(D)} \right\} \tag{2.25}$$

The dose to a volume is generally heterogeneous: so these prescriptions and tolerances are often specified as dose-to-volume-fractions, for example, that 95% of the tumor needs to receive a dose of 50 Gy (P. Metcalfe, T. Kron, and P. Hoban,2007).

Normal tissue tolerance doses might be more comprehensive, for example, according to Emami et al, a radiation-induced inflammation of the pericardium surrounding the heart has a 5% likelihood of occurring within 5 years if the entire heart receives 40 Gy, if two thirds of the heart receives 45 Gy, or if one third of the heart receives 60 Gy (AAPM Task Group 55,1995).

One way to translate the dose to a volume into a single quantity that considers the architecture of the tissue is by using equivalent uniform dose (EUD) , defined as

$$\text{EUD} = \left(\frac{1}{n} \sum_{i=1}^{n} D_i^a \right)^{\frac{1}{a}} \tag{2.26}$$

Where *N* is the number of dose points in a region of interest and is a parameter that represents the organization of the tissue (A. Niemierko,1997).

The EUD is equal to the mean dose in the structure for a=1, it tends towards the maximum dose for a > 1 (which indicates a serial architecture) and tends towards the minimum dose for a < 1 (which indicates a parallel architecture).

This means that in a tumor, for example, the equivalent uniform dose would represent the smallest dose received by a congenic FSU: providing a useful measure of the dose to the tumor that could be compared to a prescribed dose.

2.11 Treatment Planning Systems (TPSs):

Computerized treatment planning systems (TPSs) are used in external beam radiotherapy to generate beam shapes and dose distributions with the intent to maximize tumor control and minimize normal tissue complications. Patient anatomy and tumortargets can be represented as 3D models. The entire process of treatment planning involves many steps and the medical physicist is responsible for the overall integrity of the computerized TPS to accurately and reliably produce dose distributions and associated calculations for external beam radiotherapy. The planning itself is most commonly carried out by a dosimetrist, and the plan must be approved by a radiation oncologist before implementation in actual patient treatments (AAPM Task Group 55,1995).

Treatment planning prior to the 1970s was generally carried out through the manual manipulation of standard isodose charts on to patient body contours that were generated by direct tracing or lead wire representation, and relied heavily on the judicious choice of beam weight and wedging by an experienced dosimetrist.

The simultaneous development of computed tomography (CT), along with the advent of readily accessible computing power from the 1970s on, led to the development of CT based computerized treatment planning, providing the ability to view dose distributions directly superimposed upon a patient's axial anatomy. The entire treatment planning process involves many steps, beginning from beam data acquisition and entry into the computerized TPS, through patient data acquisition, to treatment plan generation and the final transfer of data to the treatment machine.

Successive improvements in treatment planning hardware and software have been most notable in the graphics, calculation and optimization aspects of current systems. Systems encompassing the 'Virtual Patient' are able to display beam's eye views (BEVs) of radiation beams and digitally reconstructed radiographs (DRRs) for arbitrary dose distributions.

Dose calculations have evolved from simple 2-D models through 3-D models to 3D Monte Carlo techniques, and increased computing power continues to increase

calculation speed. Traditional forward based treatment planning, which is based on a trial and error approach by experienced professionals, is giving way to inverse planning, which makes use of dose optimization techniques to satisfy the user specified criteria for the dose to the target and critical structures (S. Purkayastha, J. R. Milligan, and W. A. Bernhard,2006).

Dose optimization is possible by making use of dose–volume histograms (DVHs) based on CT, magnetic resonance imaging (MRI) or other digital imaging techniques. These optimized plans make use of intensity modulated radiotherapy (IMRT) to deliver the required dose to the target organ while respecting dose constraint criteria for critical organs.

Computerized treatment planning is a rapidly evolving modality, relying heavily on both hardware and software. Thus it is necessary for related professionals to develop a workable quality assurance program that reflects the use of the TPS in the clinic and that is sufficiently broad in scope to ensure proper treatment delivery.

2.11.1 TPS Software and Calculation Algorithm:

Dose calculation algorithms are the most critical software component in a computerized TPS. These modules are responsible for the correct representation of dose in the patient, and may be linked to beam time or monitor unit (MU) calculations.

Dose calculations have evolved from simple 2-D calculations, to partial 3-D point kernel methods, to full 3-D dose models in which the histories of the primary and scattered radiation in the volume of interest are considered (CUNNINGHAM,1986).

There are numerous dose calculation algorithms used by computerized TPSs, and due to the rapidly changing nature of computer power the implementation of these techniques is a constantly evolving process. Specific details of treatment planning dose algorithms can be found throughout the literature, and a small selection is included in the bibliography section of this chapter. Prior understanding sophisticated computerized treatment planning algorithms (KHAN, F.M., POTISH, R.A,1998)

.

ICRU Report No. 42 lists the chronological development of dose calculation algorithms for photon and electron beams. It provides representative examples for calculation of the central axis depth dose and the cross- beam or off-axis ratio (OAR) for photon beams. Representative examples of electron beam calculations, including the empirical and semi-empirical formalism for calculation of the central axis depth dose, and the empirical formalism for calculation of the cross-beam or OARs, are also provided.

Early TPSs generated dose distributions through the manipulation of relatively simple 2D beam data for a range of square fields in water .These data sets comprised matrices of central axis percentage depth doses (PDDs) and several OARs (profiles) at a number of depths. (CUNNINGHAM,1986)

To speed up calculation, central axis data were converted and stored as infinite PPD data, while the profiles were stored along ray lines backprojected to an arbitrary source to surface depth (SSD). In this manner, data could be rapidly manipulated using look-up tables to generate dose distributions on to external patient contours. These types of algorithm were used for both photon and electron beam treatment planning and led to very fast dose calculations. However, in general they were not truly representative of the 3D scattering conditions in the patient.

Prior to the advent and widespread CT use in treatment planning, irregular field dosimetry was accomplished using BEV films of treatment fields obtained with conventional simulators Using the central axis and profile data sets, the primary and scatter components of the beam could be separated using the zero area tissue–air ratio (TAR) and scatter–air ratio (SAR) at depth to generate Clarkson sector integration calculations for points of interest in the irregular field. (KHAN, F.M.,2003)

The approach of current beam calculation algorithms is to decompose the radiation beam into primary and secondary or scatter components, and to handle each component independently. In this manner, changes in scattering due to changes in beam shape, beam intensity, patient geometry and tissue inhomogeneities can be incorporated into the dose distribution.

One such model uses convolution methods whereby the dose at any point in the medium can be expressed as the sum of the primary and scatter components.

These models use superposition principles to account for both local changes in the primary fluence and changes in the spread of energy due to local scattering caused by the patient and beam geometry. Under specific conditions of non-divergent sources and homogeneous phantoms, convolution type integrals can be used to simplify and speed up these calculations.

Monte Carlo or random sampling techniques are used to generate dose distributions by following the histories of a large number of particles, as they emerge from the source of radiation and undergo multiple scattering interactions both inside and outside the patient.

Monte Carlo techniques are able to accurately model the physics of particle interactions by accounting for the geometry of individual linacs, beam shaping devices such as blocks and multileaf collimators (MLCs) and patient surface and density irregularities. They allow a wide range of complex patient treatment conditions to be considered.

In order to achieve a statistically acceptable result, Monte Carlo techniques require the simulation of a large number of particle histories, and are only now becoming practical for routine treatment planning as computing power reduces the calculation time to an acceptable level, of the order of a few minutes for a given treatment plan.

Pencil beam algorithms are common for electron beam dose calculations. In these techniques the energy spread or dose kernel at a point is summed along a line in a phantom to obtain a pencil type beam or dose distribution. By integrating the pencil beam over the patient's surface to account for changes in primary intensity and by modifying the shape of the pencil beam with depth and tissue density, a dose distribution can be generated. As pointed out by Cunningham, treatment planning algorithms have progressed chronologically to include analytical, matrix, semi-empirical and 3-D integration methods.

The analytical technique as developed by Sterling calculated the dose in the medium as the product of two equations, one of which modeled the PDD, while the other modeled the beam's off-axis component. The model has been extended to incorporate field shielding and wedge hardening.

Treatment planning computer systems developed in the 1970s began using the diverging matrix method of beam generation based on measured data. The Milan–Bentley model was used to calculate diverging fan lines that radiate from a source and intersect depth lines located at selected distances below the patient's surface.

Dose distributions are made by rapidly manipulating measured data sets consisting of central axis PDD and OAR data sets stored as a function of field size. These techniques continue to be used in treatment planning algorithms (Storchi and Woudstra), although they suffer from the perceived disadvantage of requiring large amounts of measured data, and from their limited ability to properly model scatter and electron transport conditions.

Semi-empirical dose calculation methods model the dose to a point by considering the contribution from the primary and scattered radiation independently. Based originally on the Clarkson scatter integration technique, these models have been refined by combining the formalism of basic physics with data derived from measurement. Correction factors to account for penumbra block transmission and flattening filters have improved in these models. These methods have been further refined by applying differential SAR techniques to allow for variations in the intensity of scatter radiation throughout the field due to the presence of wedges or non-uniform surface contours.

3D integration methods represent the transport of electrons and photons away from the primary site of interaction so as to have an accurate description of the deposition of absorbed energy while considering the geometry and composition of the entire volume being irradiated.

Monte Carlo techniques for computing dose spread arrays or kernels used in convolution–superposition methods are described by numerous authors, including Mackie, and in the review chapters in Khan and Potish, and Van Dyk provides a detailed summary of treatment planning algorithms in general.

2.11.2 Beam modifiers:

Treatment planning software for photon beams and electron beams must be capable of handling the many diverse beam modifying devices found on linac models. Some of these devices are generic to all linacs, whereas others are specific to certain manufacturers.

The travel motion (transverse or arced) will determine the junction produced by two abutted fields. The TPS will account for the penumbra produced by the location of these jaws, and differences in radial and transverse open beam symmetry due to the jaw design may also be considered.

The Blocks for Field shielding is accounted for in the TPS by considering the effective attenuation of the block to reduce the total dose under the shielded region. The dose through a partially shielded calculation volume, or voxel, is calculated as a partial sum of the attenuation proportional to the region of the voxel shielded. The geometry of straight edge and tapered blocks can be considered separately so as to more accurately model the penumbra through the region of the block edge. TPSs are able to generate files for blocked fields that can be exported to commercial block cutting machines.

The MLC is a beam shaping device that can replace almost all conventional mounted blocks, with the exception of island blocking and excessively curved field shapes. Most modern linacs are now equipped with MLCs. There are various designs; however, MLCs with a leaf width of the order of 0.5–1.0 cm at the isocenter are typical, MLCs providing smaller leaf widths are referred to as micro MLCs.

The MLC may be able to cover all or part of the entire field opening, and the leaf design may be incorporated into the TPS to model transmission and penumbra. The MLC may also have varying degrees of dynamic motion that can be invoked while the beam is on in order to enhance dose delivery.

The Static wedges remain the principal devices for modifying dose distributions. The TPS can model the effect of the dose both along and across the principal axes of the physical wedge, as well as account for any PDD change due to beam hardening and/or softening along the central axis ray line. (CUNNINGHAM,1986).

The clinical use of wedges may be limited to field sizes smaller than the maximum collimator setting. More recently, wedging may be accomplished by the use of universal or sliding wedges incorporated into the linac head, or, even more elegantly, by dynamic wedging accomplished by the motion of a single jaw while the beam is on.

Custom compensators may be designed by TPSs to account for missing tissue or to modify dose distributions to conform to irregular target shapes. TPSs are able to generate files for compensators that can be read by commercial compensator cutting machines.